

^aDepartment of Chemical and Physical Sciences, University of Toronto at Mississauga, Mississauga, ON, Canada L5L 1C6; ^bDepartment of Botany, MRC 164, Smithsonian Institution, Washington, DC 20560; ^cGeowissenschaftliches Zentrum, Universität Göttingen, D-37077 Göttingen, Germany; ^dPaläo-Ozeanographie, Ozeanzirkulation und Klimadynamik, GEOMAR Helmholtz-Zentrum für Ozeanforschung Kiel, Wischhofstr. 1-3, 24148 Kiel, Germany; ^eDepartment of Geography, Memorial University of Newfoundland, St. John's, NL, Canada A1B 3X9; and ^fDepartment of Anthropology, National Museum of Natural History, MRC 112, Smithsonian Institution, Washington, DC 20560

Northern Hemisphere sea ice has been declining sharply over the past decades and 2012 exhibited the lowest Arctic summer sea-ice cover in historic times. Whereas ongoing changes are closely monitored through satellite observations, we have only limited data of past Arctic sea-ice cover derived from short historical records, indirect terrestrial proxies, and low-resolution marine sediment cores. A multicentury time series from extremely long-lived annual increment-forming crustose coralline algal buildups now provides the first high-resolution in situ marine proxy for sea-ice cover. Growth and Mg/Ca ratios of these Arctic-wide occurring calcified algae are sensitive to changes in both temperature and solar radiation. Growth sharply declines with increasing sea-ice blockage of light from the benthic algal habitat. The 646-y multisite record from the Canadian Arctic indicates that during the Little Ice Age, sea ice was extensive but highly variable on subdecadal time scales and coincided with an expansion of ice-dependent Thule/Labrador Inuit sea mammal hunters in the region. The past 150 y instead have been characterized by sea ice exhibiting multidecadal variability with a long-term decline distinctly steeper than at any time since the 14th century.

However, the SIC-atmosphere system is especially difficult to model with only a short observational record available. Instrumental data from satellite observations have been recorded only since the late 1970s when anthropogenic effects were likely already overprinting the natural climate system. Longer-term data from historical observations are far less dependable, because coverage is patchy and reliability sometimes uncertain. For a better understanding of long-term sea-ice variability, both in space and time, a network of high-resolution multicentury or millennial-scale sea-ice data derived from proxy records are needed (3, 9). High-resolution terrestrial archives such as tree rings, varved lake sediments, and ice-core records have been

The yearly increment-forming photoautotrophic crustose coralline alga *Clathromorphum compactum*, which is widely distributed across Subarctic and Arctic coastal areas of the Northern Hemisphere (11), provides much needed annually resolved in situ sea-ice records spanning more than half a millennium. *Clathromorphum* has been calibrated as a proxy archive (12) and was subsequently used to generate multicentury-scale climate records from extratropical oceans (13). Photosynthetic *Clathromorphum* buildups have a fixed mode of life on rocky substrate and can therefore monitor and record light reaching the shallow seafloor in their high-Mg calcite skeleton. Life spans of individual plants are only limited by physical disturbance events on the seafloor, such as extreme grazing, seafloor instability, or iceberg scouring (11). Here we report on recently discovered

The most concerning example of ongoing climate change is the rapid Arctic sea-ice retreat. While just a few years ago ice-free Arctic summers were expected by the end of this century, current models predict this to happen by 2030. This shows that our understanding of rapid changes in the cryosphere is limited, which is largely due to a lack of long-term observations. Newly discovered long-lived algae growing on the Arctic sea-floor and forming tree-ring-like growth bands in a hard, calcified crust have recorded centuries of sea-ice history. The algae show that, while fast short-term changes have occurred in the past, the 20th century exhibited the lowest sea-ice cover in the past 646 years.

This article contains supporting information online at www.pnas.org/lookup/suppl/doi:10.1073/pnas.1313775110/-/DCSupplemental.

We generated individual algal proxy records by averaging normalized annual growth and Mg/Ca records from live-collected specimens from an Arctic locality characterized by an ice-free period lasting from approximately June to September and a Subarctic locality closer to the southern limit of winter sea-ice extent with an average ice-free season from May through November (Fig. 1). Algal records from both locations are significantly correlated to observational data of SIC from both satellite and ice-chart records from the 1970s onwards (Fig. 2A). At the Arctic (Subarctic) locality, up to 39% (38%) of the algal signal (1982–2007) is explained by National Snow and Ice Data Center (NSIDC)-derived SIC, and only 6% (23%) by satellite SST (21). Hence, ice cover is the dominant component driving the algal records. Much of the remaining variability can be attributed to local, as opposed to regional, temperature and particularly ice conditions distinguishing the algal records from the spatially averaged temperature and sea ice observational data (Fig. 1 shows regions used for proxy verification). An averaged record of three individual algal time series from both locations (Fig. S3) yields a long-term relationship to observational SIC data off eastern Canada (19) and the instrumental wintertime NAO for the past 150 y (20) (Fig. 2B). Modeling studies have shown that the NAO exerts an influence on the spatial distribution of winter sea ice via wind-driven anomalies of sea-ice velocity, surface vertical heat flux, and possibly horizontal oceanic heat flux (7). There is strong observational evidence connecting Arctic sea-ice distribution with the positive NAO trend from the 1960s to the early 1990s (4). At this time SIC over the Labrador Sea region and eastern Canadian Subarctic was anomalously high due to wind-driven equatorward advection of ice (7, 22), which is reflected by an interval of low growth rates and Mg/Ca ratios in the algal record (Fig. 2B). In contrast, the most dramatic increase in algal growth and Mg/Ca anomalies took place during a negative NAO phase starting in the 1920s (Fig. 2B) accompanied by strong Arctic warming and sea-ice retreat (5). An

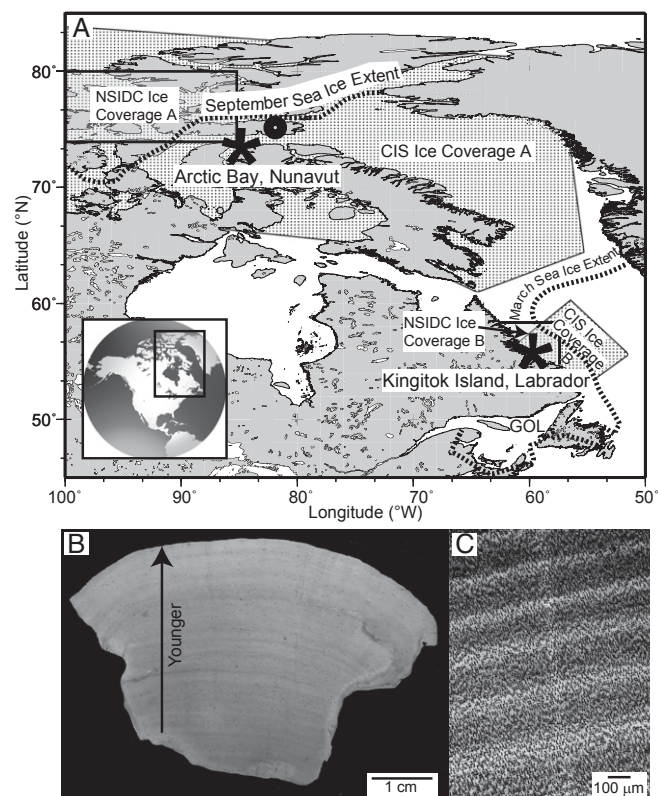


Fig. 1. (A) Locations of crustose coralline algal sea-ice proxy records (asterisks) near margins of summer and winter sea-ice extent (1979–2000 average; from NSIDC) (17). In addition, regions used for proxy verification (Fig. 2) are indicated on the map (*Methods*). Black circle indicates location of Devon Island ice core record within close proximity to Arctic Bay algal time series (18). GOL, Gulf of Saint Lawrence. (B) Polished slab of live-collected *Clathromorphum compactum* specimen. Specimen lifespan, 240 y. (C) Back-scattered electron image showing annual growth increments. White dots are individual electron microprobe elemental ratio spot measurements.

accelerated sea-ice decline starting in the 1990s is evident from both the algal proxy time series and observational data (19).

A 646-y long algal reconstruction of sea ice emphasizes the expression of the Little Ice Age (LIA) off eastern Subarctic and Arctic Canada, which is characterized by negative algal anomalies between 1530 and 1860 pointing to extensive SIC (Fig. 3). This is consistent with low Arctic temperatures (23), an increase in SIC as observed in historical accounts from Iceland and the Fram Strait (24, 25), and shown by ice core-based proxy reconstructions from Svalbard and Devon Island (18, 26). In addition, a southward migration of Thule/Labrador Inuit from Hamilton Inlet (54°N) to the northern Gulf of Saint Lawrence during the period 1500–1650 coincided with the LIA-related ice expansion that began in the early 16th century (Fig. 3). That expansion is evidenced by an increase in ice-sensitive harp seal remains found in Labrador middens and the dominance of migratory harp seals in pioneer Inuit settlement middens in the northeastern Gulf of Saint Lawrence (27). Subsistence hunting methods of the Inuit relied on ice access and may have therefore strongly benefited from the regional increase in SIC. In contrast, an overall decrease in Arctic-wide ice cover between the late 15th and early 17th century has been observed in another multiproxy-based study (3). The authors explain the declining SIC during the first half of the LIA by increased advection of warm and saline water into the eastern Arctic Ocean from the North Atlantic, a mechanism that is commonly regarded as a key element of preindustrial Arctic SIC (8). Differences between the Arctic-wide observations

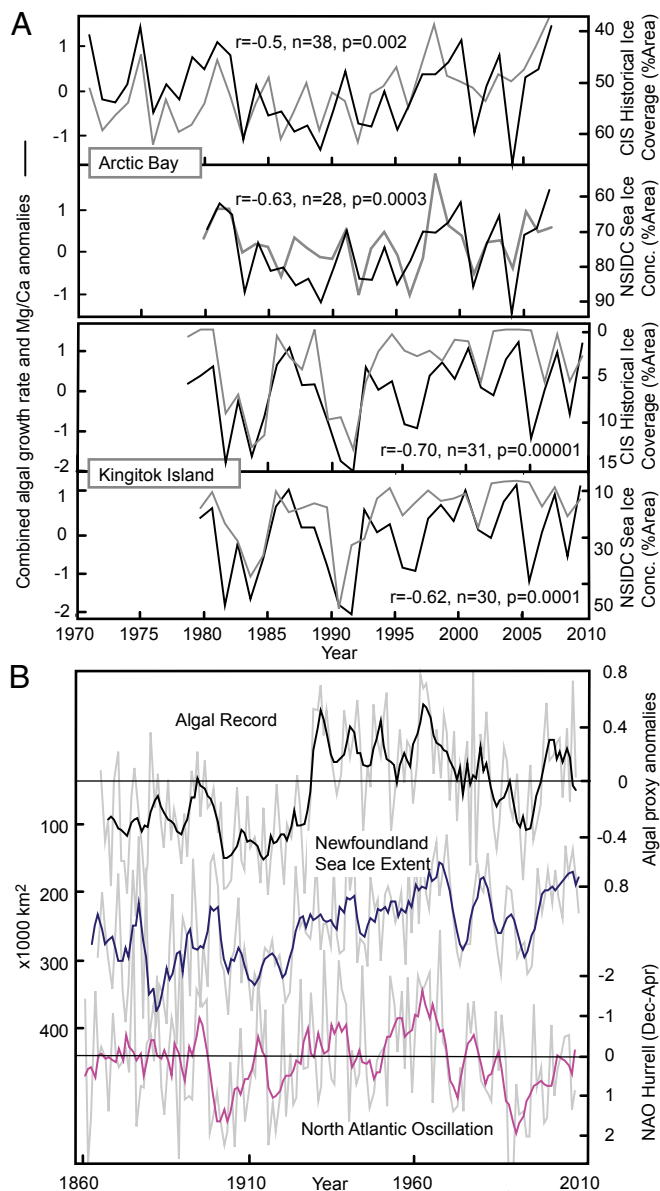


Fig. 2. Relation between sea-ice area coverage observations and crustose coralline algal proxy time series. (A) Algal proxy time series for two individual specimens [Arctic Bay (AB1) and Kingitok Island (Ki1)] compared with satellite (NSIDC) and sea-ice chart (CIS) data. Individual time series were calculated by averaging equally weighted normalized annual growth and Mg/Ca ratios of each specimen (see *Methods* for details). NSIDC data shown as July–August average from 1980 to 2007 (Arctic) and 1980–2010 (Labrador) as percent area covered by sea ice in selected region (Fig. 1). CIS data were computed for calendar week 30 and span from 1971 to 2007 in the Arctic and from 1980 to 2010 in Labrador. (B) Comparison of algal proxy time series compiled from multiple samples and locations (see *Methods* for details) to observational record of Newfoundland winter sea-ice extent (19) ($r = -0.72$, $n = 144$, $p_{\text{adj}} < 0.001$, 5-y average) and instrumental winter NAO data (20) ($r = -0.5$, $n = 144$, $p_{\text{adj}} = 0.006$, 5-y average); gray lines represent annual data, thick lines 5-y averages.

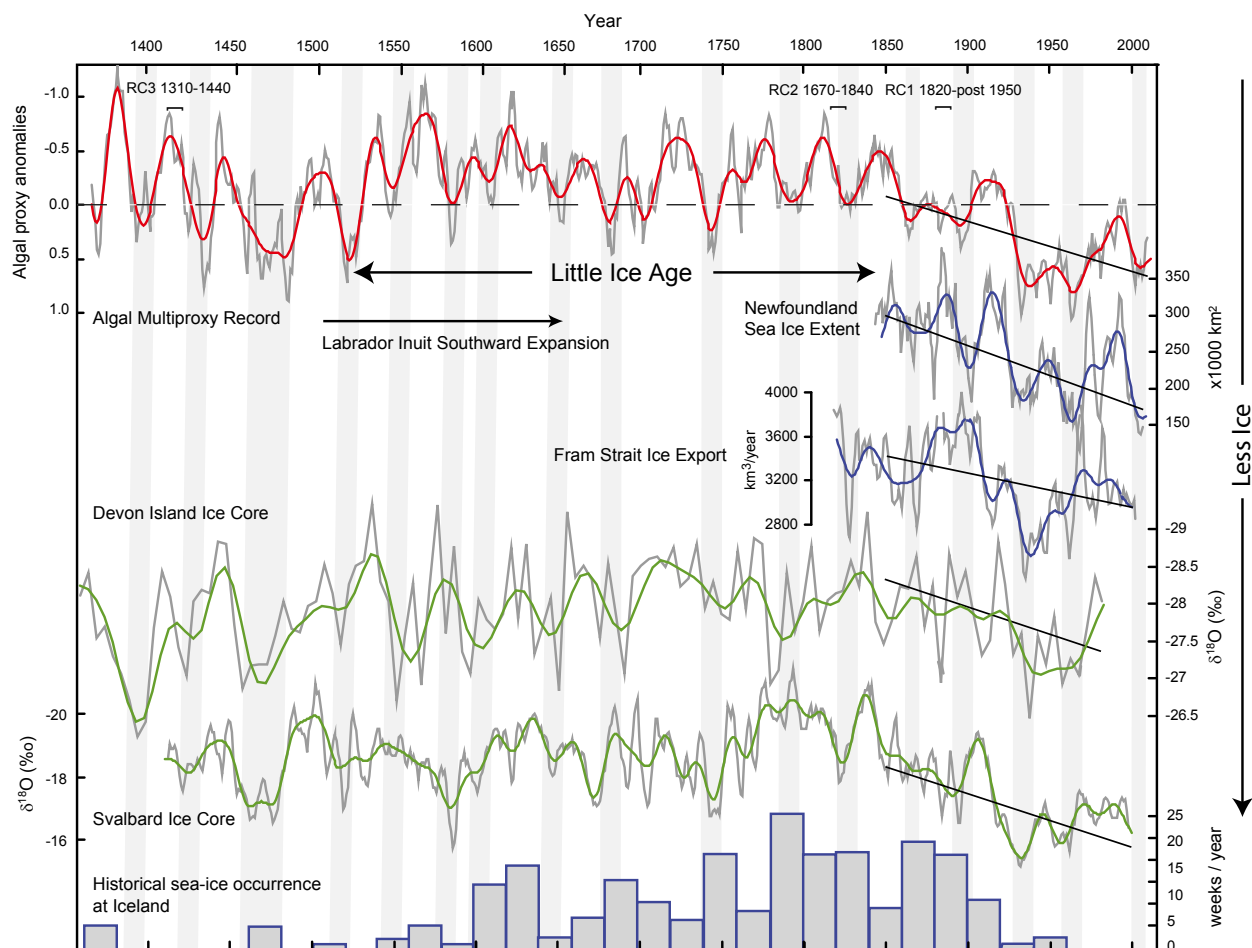
and the northeastern Canadian algal SIC record indicate that the regional variability in sea ice observed in recent decades has already existed during the LIA and highlight the asynchrony of the LIA in distinct regions globally (4, 28).

Temporal variability in the algal record can be divided into three time slices (*i*): the pre-LIA portion (1365–1530), exhibiting singular spectrum analysis (SSA) and multitaper method (MTM) spectra with dominant frequencies centered between 43 and 25 y (95%

significant), which explain 33% of the variance and frequencies between 3.5 and 5 y (11% of the variance) (Fig. S4); (ii) the LIA (1530–1860) is characterized by a combined high-frequency signal at 8 and 5.6 (99% significance, explaining 20% variance) and 37–38 y (95% significance, explaining 15%); and (iii) post-1860 multidecadal variability returns to a dominant 45- to 83-y signal (99% significance, explaining 26% of the variance). Thus, whereas multidecadal frequencies dominate the intervals of low SIC, the LIA is characterized by high-frequency variability in sea ice. A more unstable decadal-scale climate and higher-frequency sea-ice variability appear to be a feature of a cold background climate, compared with pronounced multidecadal variability during warmer intervals (29, 30). Hence, with future warming we can expect a continuation of multidecadal sea-ice variability that has dominated the Arctic since 1860. During these past 150 y, the algae have witnessed a sea-ice decline unprecedented in at least the past 646 y.

Methods

Samples of *C. compactum* were live collected at Arctic Bay, Nunavut, Canada (73.0174°N; 85.1536°W, sample AB1, 17-m depth, lifespan 1779–2009) and off Kingitok Island, Labrador, Canada (55.3983°N; 59.8467°W, sample Ki1, 17-m depth, lifespan 1851–2011; sample Ki2, 15-m depth, lifespan 1365–2011). Mg/Ca ratios were measured along transects extending over the entire lifespan of each specimen using a JEOL JXA 8900 RL electron microprobe at the University of Göttingen. For quantitative wavelength dispersive measurements, an acceleration voltage of 10 kV, a spot diameter of 3.5 μm , and a beam current of 12 nA were used. The K-alpha signals of Mg and Ca were simultaneously analyzed for 30 s on two and three spectrometers, respectively. Samples were obtained along transect lines oriented perpendicular to the plane of calcite accretion. Mg/Ca ratios were measured at 15- μm steps for specimens Ki1 and Ki2, and 10- μm steps for specimen AB1. Specimen AB1 is characterized by reduced growth rates due to its high-Arctic location, which necessitated higher-resolution sampling to achieve sub-annual sampling resolution (average of approximately six samples per year) (Fig. S3 showing individual records). At each interval the specific subsample location was selected manually by moving the stage no more than 20 μm laterally from the transect line to avoid unsuitable sample locations (i.e., conceptacles = reproductive structures and uncalcified cell interiors). The relative mean SDs of multiple standard measurements were found to be no larger than 1.0% for MgO and 1.2% for CaO (2-sigma). Counting statistics errors vary between 1.0 relative percent and 2.9 relative percent for MgO and between 0.40 relative percent and 0.62 relative percent for CaO (2-sigma). All analyzed MgO concentrations clearly exceed the detection limit, which, calculated from the background noise, was 0.015% (2-sigma). Age models were established based on the pronounced seasonal cycle in algal Mg/Ca as discussed in Halfar et al. (14). Maximum (minimum) Mg/Ca values of subannual cycles were tied to August (March), which is on average the warmest (coolest) month in the study area. Minimum Mg/Ca values represent the winter growth break, which was assigned to the maximum extent of the sea-ice season (March). Mg/Ca time series were linearly interpolated between these anchor points using AnalySeries software (31) to obtain an equidistant proxy time series with 12 samples per year resolution. The developed chronology was refined and thoroughly cross-checked for possible errors in the age model by comparing annual extreme values in the Mg/Ca ratio time series to imaged growth increment patterns for each individual year of algal growth. In addition, the age model was confirmed by three accelerator mass spectrometry (AMS) radiocarbon dates obtained from sample Ki2 (Fig. 3 shows position of dates and Table S1, analytical details). Once an age model was finalized, annual average Mg/Ca ratios were calculated from the 12 samples per year dataset. In addition, widths of annual Mg/Ca cycles were determined by calculating the distance between microprobe stage coordinates of successive Mg/Ca lows. Widths of annual Mg/Ca cycles are equivalent to annual vertical growth rates (14). Error of growth measurement is dependent on microprobe sampling resolution (e.g., 15 μm for Ki1 and Ki2, 10 μm for AB1). As collections took place during the summer months, the year of collection is incomplete and counting was done starting from the year before collection. Individual reconstructions were standardized to have a mean of zero and unit variance. A combined algal record (Fig. 3) was calculated by averaging the normalized annual growth rates and annually averaged Mg/Ca ratios from all three samples, giving equal weight to each of the time series (Fig. S3 showing individual records). Regions used for proxy calibration (Fig. 2A): NSIDC ice coverage time series were obtained as summer average (July–August) of sea-ice concentrations



derived from satellite brightness data (17). NSIDC regions were selected based on spatial correlations of proxy records with ice-coverage data. Region A encompasses 74–80°N, 85–100°W; region B encompasses 54–57°N, 57–62°W. Canadian Ice Service (CIS) time series were compiled from weekly regional ice charts from predefined regions (A, northern Canadian water; B, southern Labrador) using Ice Graph (32). SST data were obtained from Reynolds et al. (21). Newfoundland winter sea-ice extent (Fig. 2B) was derived from historical and observational records (19). Historical observations and modeled data of Fram Strait ice export from Schmith and Hansen (24). Svalbard Austfonna $\delta^{18}\text{O}$ ice core record has been interpreted

as sea-ice extent proxy (26), whereas Devon Island ice core $\delta^{18}\text{O}$ record (Fig. 1 for location) shows correlation with sea-ice conditions at decadal timescales only (3). Historical record of sea-ice occurrence off Iceland was modified from Lamb (25).

ACKNOWLEDGMENTS. W. Kuhs stimulated our interest in ice-cover proxy development. Funding was provided by Estech (Ecological Systems Technology) (to W.H.A.), National Science and Engineering Research Council (to J.H. and E.E.), a Canadian Foundation for Climate and Atmospheric Sciences Grant (to J.H.), an ArcticNet Network of Centres of Expertise Grant (to E.E.), and the Smithsonian Institution (to W.H.A. and W.W.F.).

- de Vernal A, Gersonde R, Goosse H, Seidenkrantz M-S, Wolff EW (2013) Sea ice in the paleoclimate system: The challenge of reconstructing sea ice from proxies—an introduction. *Quat Sci Rev*, 10.1016/j.quascirev.2013.08.009.
- Abram NJ, Wolff E, Curran MAJ (2013) A review of the sea ice proxy information from polar ice cores. *Quat Sci Rev*, 10.1016/j.quascirev.2013.01.011.
- Kinnard C, et al. (2011) Reconstructed changes in Arctic sea ice over the past 1,450 years. *Nature* 479(7374):509–512.
- Grumet N, et al. (2001) Variability of sea-ice extent in Baffin Bay over the last millennium. *Clim Change* 49:129–145.
- Semenov VA, Bengtsson L (2003) Modes of the wintertime Arctic temperature variability. *Geophys Res Lett* 30(15):1781–1784.
- Rodrigues J (2008) The rapid decline of sea ice in the Russian Arctic. *Cold Reg Sci Technol* 54(2):124–142.
- Strong C, Magnusdottir G (2010) Modeled winter sea ice variability and the North Atlantic Oscillation: A multi-century perspective. *Clim Dyn* 34:515–525.
- Spielhagen RF, et al. (2011) Enhanced modern heat transfer to the Arctic by warm Atlantic Water. *Science* 331(6016):450–453.
- Gersonde R, de Vernal A (2013) Reconstruction of past sea ice extent. *PAGES News* 21 (1):30–31.
- Polyak L, et al. (2010) History of sea ice in the Arctic. *Quat Sci Rev* 29:1757–1778.
- Adey WH, Halfar J, Williams B (2013) The coralline genus *Clathromorphum* Foslée emend. Adey: Biological, physiological, and ecological factors controlling carbonate production in an Arctic-Subarctic climate archive. *Smithsonian Contributions to the Marine Sciences* (Smithsonian Institution Scholarly Press, Washington, DC), Vol 40, pp 1–48.
- Halfar J, Steneck RS, Joachimski M, Kronz A, Wanamaker AD, Jr. (2008) Coralline red algae as high-resolution climate recorders. *Geology* 36:463–466.
- Hetzinger S, et al. (2012) First proxy evidence linking decadal North Pacific and Atlantic climate. *Clim Dyn* 39(6):1447–1455.
- Halfar J, et al. (2011) Coralline algal growth-increment widths archive North Atlantic climate variability. *Palaeogeogr Palaeoclimatol Palaeoecol* 302:71–80.
- Halfar J, et al. (2011) 225 years of Bering Sea climate and ecosystem dynamics revealed by coralline algal growth-increment widths. *Geology* 39(6):579–582.
- Reynolds RW, Smith TM (1994) Improved global sea surface temperature analyses using optimum interpolation. *J Clim* 7:929–948.

17. Meier W, Fetterer F, Knowles K, Savoie M, Brodzik MJ (2006, updated quarterly) Sea ice concentrations from Nimbus-7 SMMR and DMSP SSM/I passive microwave data (National Snow and Ice Data Center, Boulder, CO), 1980–2011.
18. Kinnard C, Zdanowicz CM, Fisher DA, Wake CP (2006) Calibration of an ice-core glaciochemical (sea-salt) record with sea-ice variability in the Canadian Arctic. *Ann Glaciol* 44:383–390.
19. Hill BT, Jones SJ (1990) The Newfoundland ice extent and the solar cycle from 1860 to 1988. *Journal of Geophysical Research* 95:5385–5394.
20. Hurrell JW (1995) Decadal trends in the North Atlantic Oscillation: Regional temperatures and precipitation. *Science* 269(5224):676–679.
21. Reynolds RW, Rayner NA, Smith TM, Stokes DC, Wang W (2002) An improved in situ and satellite SST analysis for climate. *J Clim* 15:1609–1625.
22. Chapman WL, Walsh JE (1993) Recent variations of sea ice and air temperature in high latitudes. *Bull Am Meteorol Soc* 74(1):33–47.
23. Kaufman DS, et al.; Arctic Lakes 2k Project Members (2009) Recent warming reverses long-term arctic cooling. *Science* 325(5945):1236–1239.
24. Schmith T, Hansen C (2003) Fram Strait ice export during the nineteenth and twentieth centuries reconstructed from a multiyear sea ice index from southwestern Greenland. *J Clim* 16:2781–2791.
25. Lamb HH (1977) Climate history and the future. *Climate: Present, Past and Future* (Methuen, London), Vol 2.
26. Isaksson E, et al. (2005) Two ice-core $d^{18}O$ records from Svalbard illustrating climate and sea-ice variability over the last 400 years. *Holocene* 15:501–509.
27. Fitzhugh WW (2006) Cultures, borders, and basques: Archaeological surveys on Quebec's lower north shore. *From the Arctic to Avalon: Papers in Honour of James A Tuck Jr.*, eds Rankin L, Ramsden P, British Archaeological Reports International Series (Archaeopress, Oxford, London), 1507:53–70.
28. Ahmed M; PAGES 2k Consortium (2013) Continental-scale temperature variability during the past two millennia. *Nature Geosc* 6:339–346.
29. Chylek P, Folland CK, Dijkstra HA, Lesins G, Dubey MK (2011) Ice-core data evidence for a prominent near 20 year time-scale of the Atlantic Multidecadal Oscillation. *Geophys Res Lett* 38:L13704.
30. Kobashi T, et al. (2009) Persistent multi-decadal Greenland temperature fluctuation through the last millennium. *Clim Change* 100:733–756.
31. Paillard D, Labeyrie L, Yiou P (1996) Macintosh program performs time-series analysis. *Eos Trans AGU* 77:379.
32. Tivy A, et al. (2011) Trends and variability in summer sea ice cover in the Canadian Arctic based on the Canadian Ice Service Digital Archive. *J Geophys Res* 116(C03007): 10.1029/2009JC005855.